Compensating for visco-acoustic effects in TTI reverse time migration

Yi Xie, James Sun, Yu Zhang, Joe Zhou, CGG

Summary

Anelastic effects of the overburden cause seismic amplitude attenuation, wavelet phase distortion and seismic resolution reduction. It is desirable to correct the frequency dependent energy attenuation and phase distortion within a prestack depth migration. The situation becomes more challenging in complex geological regions which host absorption effects such as shallow gas clouds. The wavefields can be severely complicated and distorted by strong velocity contrasts and significant attenuation, hence masking the image of deeper targets. To deal with such challenges associated with absorption in complex geological regions, which need to account for multi-pathing and anisotropy in wave propagation, we have developed a stable visco-acoustic TTI reverse time migration (RTM). This is based on a formulation we derived for visco-acoustic wave propagation in a TTI medium to compensate for the anelastic effects in seismic data. We will demonstrate our visco-acoustic TTI RTM with both synthetic and field data examples.

Introduction

It has been observed that the anelastic effects of the earth cause seismic energy attenuation and wavelet distortion (Aki and Richards, 1980). For example, gas trapped in overburden structures can strongly attenuate seismic P-waves. As a result, not only is the migrated amplitude below the gas anomaly dim, but also the imaging resolution is greatly reduced due to the high frequency energy loss and the phase distortion. Thus, there is a need to compensate for the absorption effects in seismic processing to make the final image more interpretable.

Early work to compensate for seismic absorption was performed in the data domain by an inverse Q-filter (e.g., Kjartansson, 1979; Bickel and Natarajan, 1985; Hargreaves and Calvert, 1991). These methods are based on a one-dimensional backward propagation and cannot correctly handle real geological complexity. Since anelastic attenuation and dispersion happen during the wave propagation, it is natural to correct them in a prestack depth migration. However, most migration methods usually treat the earth model as a lossless acoustic medium and only intend to correct for the amplitude effect due to geometric spreading (Bleistein et al., 2001). Mainly two reasons account for this situation. First, it is difficult to accurately estimate the Q factor from seismic data. Second, the technology of migrating seismic data using a visco-acoustic equation or an anelastic equation has not been well established.

Xin et al. (2008) have developed a generalized method for estimating absorption losses. The analysis is performed on migrated data and based on the tomographic velocity updating algorithm described by Zhou et al. (2003). Xie et al. (2009, 2010) have developed an efficient approach for compensation of frequency dependent dissipation effects in Kirchhoff and Gaussian beam prestack depth migration making use of the absorption model estimated from a 3D tomographic amplitude inversion. It applies Q compensation during migration, fully honoring actual raypaths.

Some effort has been made to develop an inverse Q-migration using one-way wave equation migration (Dai and West, 1994; Yu et al., 2002). The one-way wave equation is formulated in the frequency domain which means it is straightforward to take care of the frequency dependent dissipation. RTM based on directly solving the two-way wave equation provides a superior way to image complex geologic regions and has become a standard migration tool for subsalt imaging, especially in the Gulf of Mexico. To incorporate an attenuation correction within RTM, we need to formulate a time domain wave equation to model the visco-acoustic effects. Zhang et al. (2010) derived a pseudo-differential equation to model isotropic visco-aoustic waves based on the dispersion relation and apply it to reverse time migration to compensate for anelastic effects in seismic images. However, it turns out to be a difficult task to extend Zhang's approach to formulate visco-acoustic TTI RTM.

Alternatively, a visco-elastic mechanical model consisting of standard linear solids (SLSs) has been proposed to model real earth materials and employed to solve the visco-elastic wave equation for forward modeling (Robertsson et al., 1994). One SLS consists of a spring in parallel with a spring and a dashpot in series. It can approximate a constant Q within a defined frequency band with a series of SLSs connected in parallel (Day and Minster, 1984). In an SLS the stress-strain relationship is expressed as a causal time convolution of a stress relaxation function with the strain rate. This time dependence of the relaxation mechanism is governed by the stress and strain relaxation times. Liu et al. (1976) showed that a visco-elastic rheology with multiple relaxation mechanisms can explain experimental observations of wave propagations in the earth. Carcione et al. (1988) designed a system of equations of motion and introduced memory variables to obviate storing the entire strain history required by the time convolution. This visco-acoustic wave propagation based on multiple relaxation mechanisms can be extended to

DOI http://dx.doi.org/10.1190/segam2015-5855445.1

account for anisotropy; however, the time reversal propagation is unstable, which poses challenges in implementing visco-acoustic TTI RTM.

In this paper, we will describe a stable visco-acoustic TTI RTM scheme based on a formulation we derived for visco-acoustic wave propagation in TTI anisotropic media. We will demonstrate our visco-acoustic TTI RTM with both synthetic and field data examples from offshore Southeast Asia, where complex gas pockets in the overburden pose challenges in the imaging for the underneath objectives.

Method

Based on the relation between stress and strain in the case of linear visco-elasticity, we derive the visco-acoustic wave equation in a TTI anisotropic medium as follows,

$$(i\omega)^{2-2\gamma}\begin{pmatrix} p \\ r \end{pmatrix} = \frac{v_0^2 \cos^2\frac{\pi\gamma}{2}}{\omega_0^{2\gamma}}\begin{pmatrix} 1+2\varepsilon & \sqrt{1+2\delta} \\ \sqrt{1+2\delta} & 1 \end{pmatrix}\begin{pmatrix} G_{xx}+G_{yy} & 0 \\ 0 & G_{zz} \end{pmatrix}\begin{pmatrix} p \\ r \end{pmatrix} \tag{1}$$

where $p(\vec{x},t)$ is the wavefield at the imaging point in the subsurface $\vec{x}$, $v(\vec{x})$ is velocity field, the Thomsen anisotropy parameters are ε and δ, $\gamma(\vec{x}) = 1/(\pi Q)$ is the absorption coefficient, and ω_0 is the reference frequency. G_{xx}, G_{yy} and G_{zz} are rotated differential operators, for example, $G_{xx} = (D_x)^T(D_x)\cdot$ $(D_{\vec{x}})^T$ is the transpose of the operator D_x, and $D_x = \frac{\partial}{\partial x}\cos\varphi\cos\theta + \frac{\partial}{\partial y}\sin\varphi\cos\theta - \frac{\partial}{\partial z}\sin\theta\cdot$ θ and φ are the tilt angle and the azimuth of the tilt of the TTI symmetry axis, respectively. $v_0(\vec{x})$ is the velocity field at the reference frequency. $r(\vec{x},t)$ is the auxiliary wavefield. We approximate the fractional derivative by the Lth order generalized Maxwell bodies,

$$(i\omega)^{-2\gamma} \approx 1 + \sum_{l=1}^{L}\frac{c_l}{i\omega+\omega_l} \tag{2}$$

where ω_l are the relaxation frequencies and c_l are the weight factors of the classical Maxwell bodies, which form the generalized Maxwell body. Thus, the visco-acoustic TTI wave equations can be reformulated in the time domain as

$$\begin{cases} \frac{\partial^2}{\partial t^2}\begin{pmatrix} p \\ r \end{pmatrix} + \sum_{l=1}^{L}\frac{\partial^2}{\partial t^2}\begin{pmatrix} d_l \\ e_l \end{pmatrix} = \frac{v_0^2\cos^2\frac{\pi\gamma}{2}}{\omega_0^{2\gamma}}\begin{pmatrix} 1+2\varepsilon & \sqrt{1+2\delta} \\ \sqrt{1+2\delta} & 1 \end{pmatrix}\begin{pmatrix} G_{xx}+G_{yy} & 0 \\ 0 & G_{zz} \end{pmatrix}\begin{pmatrix} p \\ r \end{pmatrix} \\ \omega_l\begin{pmatrix} d_l \\ e_l \end{pmatrix} + \frac{\partial}{\partial t}\begin{pmatrix} d_l \\ e_l \end{pmatrix} = c_l\begin{pmatrix} p \\ r \end{pmatrix} \end{cases} \tag{3}$$

where d_l and e_l are the memory variables.

Time marching using equation (3) will forward propagate the wavefield in an anisotropic visco-acoustic medium; the wavefield will experience frequency dependent attenuation through the propagation. Visco-acoustic RTM requires a time reversed propagation of the receiver wavefield. Unfortunately, the time reversal propagation using equation (3) turns out to be unstable. To overcome the instability issue, we propose a new scheme using the anisotropic wave equation in a so-called conjugate medium:

$$\begin{aligned} &(i\omega)^2(\omega)^{-2\gamma}(\cos\pi\gamma + i\sin\pi\gamma)\begin{pmatrix} u \\ w \end{pmatrix} \\ &= \frac{v_0^2\cos^2\frac{\pi\gamma}{2}}{\omega_0^{2\gamma}}\begin{pmatrix} 1+2\varepsilon & \sqrt{1+2\delta} \\ \sqrt{1+2\delta} & 1 \end{pmatrix}\begin{pmatrix} G_{xx}+G_{yy} & 0 \\ 0 & G_{zz} \end{pmatrix}\begin{pmatrix} u \\ w \end{pmatrix} \end{aligned} \tag{4}$$

where $u(\vec{x},t)$, $w(\vec{x},t)$ are the wavefield and the auxiliary wavefield, respectively.

The conjugate medium will honour the same phase velocity as the original visco-acoustic medium, while the time reversal propagation of equation (4) will attenuate rather than boost the wavefield in its propagation from the reveivers back to the reflectors. We compute the desired backward propagated receiver wavefield $\tilde{p}(\vec{x},\omega)$ at each subsurface imaging point $\vec{x}$ by the following amplitude spectrum compensation:

$$\tilde{p}(\vec{x},\omega) = \left|\frac{\tilde{p}_a(\vec{x},\omega)}{\tilde{w}(\vec{x},\omega)}\right|^2 \tilde{w}(\vec{x},\omega) \tag{5}$$

where $\tilde{w}(\vec{x},\omega)$ is the wavefield obtained by solving equation (4), and $\tilde{p}_a(\vec{x},\omega)$ is the wavefield obtained by solving the acoustic TTI wave equation in a lossless medium:

$$\begin{aligned} &(i\omega)^2\begin{pmatrix} p_a \\ r_a \end{pmatrix} \\ &= \frac{v_0^2\cos^2\frac{\pi\gamma}{2}}{\omega_0^{2\gamma}}\begin{pmatrix} 1+2\varepsilon & \sqrt{1+2\delta} \\ \sqrt{1+2\delta} & 1 \end{pmatrix}\begin{pmatrix} G_{xx}+G_{yy} & 0 \\ 0 & G_{zz} \end{pmatrix}\begin{pmatrix} p_a \\ r_a \end{pmatrix} \end{aligned} \tag{6}$$

where $r_a(\vec{x},t)$ is the corresponding auxiliary wavefield in the acoustic TTI wave equation.

Examples

We first show an impulse response test in Figure 1. One single trace contained in the input seismic data with shot and receiver co-located at the central subline 161 and central crossline 161 with 7 Hz Ricker wavelet put at time

DOI http://dx.doi.org/10.1190/segam2015-5855445.1

1 s, 2 s and 3 s, respectively. The medium has a constant velocity of 2000 m/s. Figure 1(*a*) shows the impulse response from conventional TTI reverse time migration. We then apply frequency dependent absorption to the single trace seismic input, constant Q=100, reference frequency 100 Hz. Figure 1(*b*) is the impulse response of the input data with absorption, but still migrated by conventional TTI reverse time migration. The amplitudes are attenuated and the phase is distorted as the velocity varies with frequency. We then migrate the input data with absorption using our proposed visco-acoustic TTI reverse time migration. Figure 1(*c*) shows the Q TTI RTM impulse response which agrees well with the result in Figure 1(*a*), indicating that our Q TTI RTM successfully compensates for the absorption effects. Figure 1(*d*) compares the spectrum. Q TTI RTM compensates for attenuation in a frequency dependent manner.

We also applied our method to a field data set from offshore Southeast Asia. Complex gas pockets in the overburden challenge the imaging of deeper targets. Figure 2 shows the velocity model and the absorption anomalies estimated using Q tomographic inversion. Figures 3(*a*) and 3(*b*) compare the section from conventional Kirchhoff TTI PSDM and conventional TTI RTM. RTM handles multi-pathing due to the strong velocity contrast of gas clouds with the surrounding sediments, giving a better image than Kirchhoff PSDM. However, amplitude dimming caused by gas in the shallow region was observed in both the Kirchhoff PSDM and RTM sections. The amplitude loss makes it difficult to identify and interpret reflectors. We then utilized the estimated absorption anomalies in both 3D Q Kirchhoff PSDM and Q TTI RTM to mitigate the dissipation effects, as depicted in Figures 3(*c*) and 3(*d*). The amplitudes are more balanced after the correction, and the resolution is also increased. We observe that the amplitudes of events underneath the shallow gas are restored, wavelets are sharper, and the continuity is improved. Comparing Kirchhoff Q PSDM and Q TTI RTM, they both compensate for the amplitude attenuation, phase distortion and resolution reduction due to the absorption of shallow gas. However, the events underneath the complex shallow gas are clearer, more continuous and stronger in the Q TTI RTM image, attributed to the multi-pathing capability of Q TTI RTM.

Conclusions

We have developed Q TTI RTM with compensation for frequency dependent dissipation effects caused by absorption in the overburden. Synthetic and real data results show that our method can successfully compensate for the amplitude loss and phase distortion associated with absorption anomalies. For areas where complex gas clouds are a common phenomenon, this Q TTI RTM technique presents a solution to the challenge of revealing and imaging hydrocarbon reservoirs beneath attenuative media by handling both multi-pathing and absorption in wave propagation.

Acknowledgements

We thank CGG for permission to publish this work. We thank Xiaodong Wu, Nina Lim, and Zhiyuan Wei for the field data examples. We thank Dechun Lin for his support and insightful discussions.

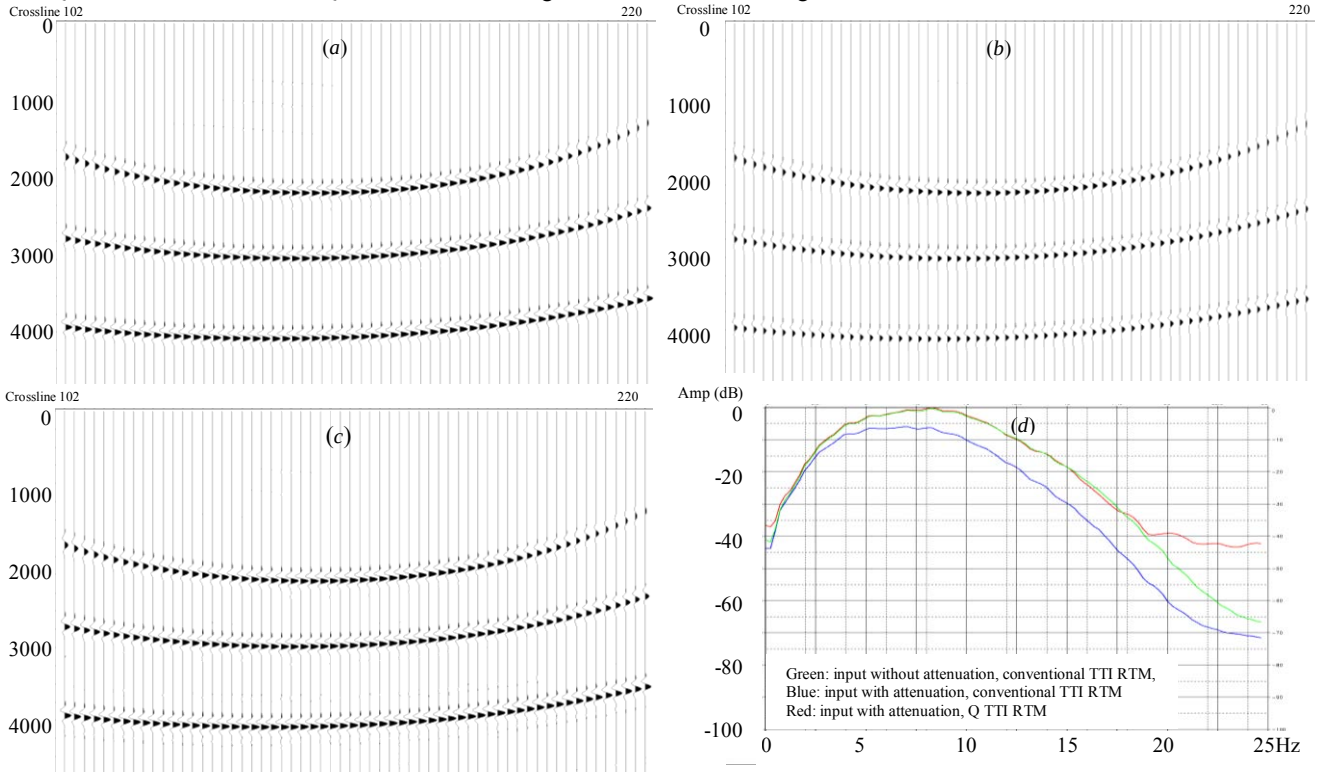

Figure 1: Impulse response comparison. (a) input without attenuation, conventional TTI RTM, (b) input with attenuation, conventional TTI RTM, (c) input with attenuation, Q TTI RTM, (d) comparison of spectrum.

DOI http://dx.doi.org/10.1190/segam2015-5855445.1

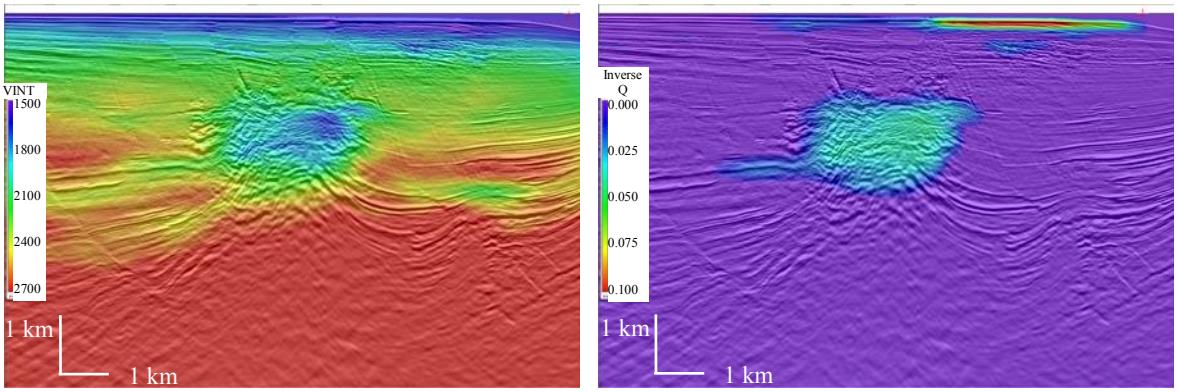

(*a*) (*b*)

Figure 2: The models overlaid on PSDM imaging. (*a*): velocity model; (*b*): absorption model from Q tomography.

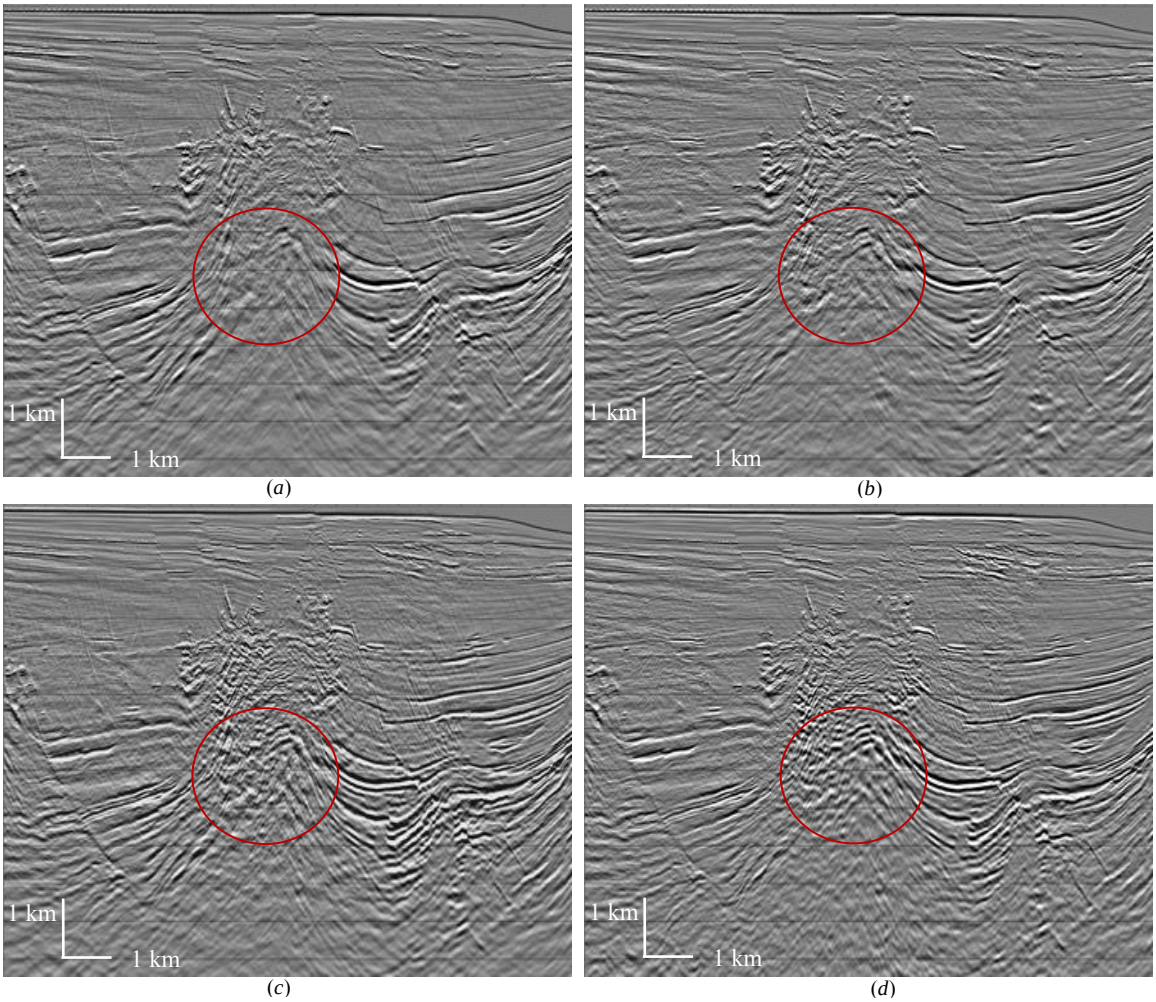

(*a*) (*b*)

(*c*) (*d*)

Figure 3: Comparison of Kirchhoff TTI PSDM (*a*), TTI RTM (*b*), Kirchhoff Q TTI PSDM (*c*) and Q TTI RTM (*d*) in the TTI attenuative medium.

DOI http://dx.doi.org/10.1190/segam2015-5855445.1

EDITED REFERENCES

Note: This reference list is a copyedited version of the reference list submitted by the author. Reference lists for the 2015 SEG Technical Program Expanded Abstracts have been copyedited so that references provided with the online metadata for each paper will achieve a high degree of linking to cited sources that appear on the Web.

REFERENCES

Aki, K., and P. G. Richards, 1980, Quantitative seismology: W.H. Freeman & Co.

Bickel, S. H., and R. R. Natarajan, 1985, Plane-wave Q deconvolution: Geophysics, **50**, 1426–1439. http://dx.doi.org/10.1190/1.1442011.

Bleistein, N., J. W. Stockwell, and J. K. Cohen, 2001, Mathematics of multidimensional seismic inversion: Springer Publishing Co. http://dx.doi.org/10.1007/978-1-4613-0001-4.

Carcione, J. M., D. Kosloff, and R. Kosloff, 1988, Viscoacoustic wave propagation simulation in the earth: Geophysics, **53**, 769–777. http://dx.doi.org/10.1190/1.1442512.

Dai, N., and G. F. West, 1994, Inverse Q-migration: 64th Annual International Meeting, SEG, Expanded Abstracts, 1418–1421.

Day, S. M., and J. B. Minster, 1984, Numerical simulation of attenuated wavefields using a Pade approximation method: Geophysical Journal of the Royal Astronomy Society, **78**, 105–118.

Hargreaves, N. D., and A. J. Calvert, 1991, Inverse Q-filtering by Fourier transform: Geophysics, **56**, 519–527. http://dx.doi.org/10.1190/1.1443067.

Kjartansson, E., 1979, Constant Q-wave propagation and attenuation: Journal of Geophysical Research, **84**, B9, 4737–4748. http://dx.doi.org/10.1029/JB084iB09p04737.

Liu, H. P., D. L. Anderson, and H. Kanamori, 1976, Velocity dispersion due to anelasticity: Implications for seismology and mantle composition: Geophysical Journal of the Royal Astronomy Society, **47**, no. 1, 41–58. http://dx.doi.org/10.1111/j.1365-246X.1976.tb01261.x.

Robertsson, J. O. A., J. O. Blanch, and W. W. Symes, 1994, Viscoelastic finite-difference modeling: Geophysics, **59**, 1444–1456. http://dx.doi.org/10.1190/1.1443701.

Ruppel, C., R. Boswell, and E. Jones, 2008, Scientific results from Gulf of Mexico gas hydrates joints industry project leg 1 drilling: Introduction and overview: Marine and Petroleum Geology, **25**, no. 9, 819–829. http://dx.doi.org/10.1016/j.marpetgeo.2008.02.007.

Xie, Y., C. Notfors, J. Sun, K. Xin, A. Biswal and M. Balasubramaniam, 2010, 3D prestack beam migration with compensation for frequency dependent absorption and dispersion: Presented at the 72nd Annual International Conference and Exhibition, EAGE.

Xie, Y., K. Xin, J. Sun, and C. Notfors, 2009, 3D prestack depth migration with compensation for frequency dependent absorption and dispersion: 79th Annual International Meeting, SEG, Expanded Abstracts, 2919–2922.

Xin, K., B. Hung, S. Birdus, and J. Sun, 2008, 3D tomographic amplitude inversion for compensating amplitude attenuation in the overburden: 78th Annual International Meeting, SEG, Expanded Abstracts, 3239–3243.

Yu, Y., R. S. Lu, and M. D. Deal, 2002, Compensation for the effects of shallow gas attenuation with viscoacoustic wave-equation migration: 72nd Annual International Meeting, SEG, Expanded Abstracts, 2062–2065.

Zhang, Y., and J. Sun, 2009, Practical issues of reverse time migration: True-amplitude gathers, noise removal and harmonic-source encoding: First Break, 26, 19–25.

DOI http://dx.doi.org/10.1190/segam2015-5855445.1

Zhang, Y., P. Zhang, and H. Zhang, 2010, Compensating for visco-acoustic effects in reverse-time migration: 80th Annual International Meeting, SEG, Expanded Abstracts, 3160–3164.

Zhou, H., S. Gray, J. Young, D. Pham, and Y. Zhang, 2003, Tomographic residual curvature analysis: The process and its components: 73rd Annual International Meeting, SEG, Expanded Abstracts, 666–669.

DOI http://dx.doi.org/10.1190/segam2015-5855445.1